Theses and Dissertations | 1. Thesis and Dissertation Collection, all items

1995-06

The effects of a klyston on a high-current, high-gain free electron laser at SLAC

Winter, Gordon H.

Monterey, California. Naval Postgraduate School

http://hdl.handle.net/10945/7524

NAVAL POSTGRADUATE SCHOOL
MONTEREY, CALIFORNIA

THESIS

THE EFFECTS OF A KLYSTRON ON A HIGH-CURRENT, HIGH-GAIN FREE ELECTRON LASER AT SLAC

by

Gordon H. Winter

June, 1995

Thesis Advisor: W.B. Colson

REPORT DOCUMENTATION PAGE

Form Approved OMB No. 0704-0188

1. AGENCY USE ONLY *(Leave blank)*	2. REPORT DATE June , 1995	3. REPORT TYPE AND DATES COVERED Master's Thesis

4. TITLE AND SUBTITLE THE EFFECTS OF A KLYSTRON ON A HIGH-CURRENT, HIGH-GAIN FREE ELECTRON LASER AT SLAC	5. FUNDING NUMBERS
6. AUTHOR(S) Winter, Gordon H.	

7. PERFORMING ORGANIZATION NAME(S) AND ADDRESS(ES) Naval Postgraduate School Monterey CA 93943-5000	8. PERFORMING ORGANIZATION REPORT NUMBER

9. SPONSORING/MONITORING AGENCY NAME(S) AND ADDRESS(ES)	10. SPONSORING/MONITORING AGENCY REPORT NUMBER

11. SUPPLEMENTARY NOTES The views expressed in this thesis are those of the author and do not reflect the official policy or position of the Department of Defense or the U.S. Government.

12a. DISTRIBUTION/AVAILABILITY STATEMENT Approved for public release; distribution is unlimited.	12b. DISTRIBUTION CODE

13. ABSTRACT *(maximum 200 words)*

A high-current, high-power X-ray Free Electron Laser (FEL) using the Stanford linear accelerator (SLAC) as an electron beam source has been proposed. Such a system will provide the scientic community with its first realistic X-ray laser. One dramatic use a hard X-ray laser light at the proposed wavelength of 1.5 Angstrom would be to image DNA base-pairs [7].

   With an accelerator already in place, the major cost of developing the SLAC system would be in the manufacturing of the undulator. The cost in building an undulator is proportional to its length. This thesis uses numerical simulation to evaluate the effectiveness of an FEL klystron in order to decrease the length of the undulator with a dispersive section. Simulations show that the quality of the electron beam injected into the undulator can greatly effect the ability of an FEL to produce coherent light, and is a factor in determining the length of the undulator needed for saturation. In the high-gain FEL (such as proposed at SLAC), a dispersive section is sensitive to energy spread and may adversely affect the gain of the system. For moderate to low energy spread, it is found that a klystron is useful in shortening the undulator length.

   By examining how the strength of a klystron dispersive section affects the gain of a high-current system, we determine a critical strength above which the klystron can be detrimental. A dispersive section that is either too strong or not strong enough will result in less than optimum gain, or an increase in the required length of an undulator.

   Single-mode, phase-space simulations are used to visualize the effect on electron bunching and the onset of saturation. Longitudinal multimode simulations show the resulting coherence development.

14. SUBJECT TERMS Free Electron Laser, High-Current, High-Gain, Klystron, Undulator		15. NUMBER OF PAGES 58
		16. PRICE CODE

17. SECURITY CLASSIFICATION OF REPORT Unclassified	18. SECURITY CLASSIFICATION OF THIS PAGE Unclassified	19. SECURITY CLASSIFICATION OF ABSTRACT Unclassified	20. LIMITATION OF ABSTRACT UL

THE EFFECTS OF A KLYSTON ON A HIGH-CURRENT, HIGH-GAIN FREE ELECTRON LASER AT SLAC

Gordon H. Winter
Lieutenant, United States Navy
B.S., University of Utah, 1987

Submitted in partial fulfillment
of the requirements for the degree of

MASTER OF SCIENCE IN PHYSICS

from the

NAVAL POSTGRADUATE SCHOOL
June 1995

Author: ███████████████████████
Gordon H. Winter

Approved by: ███████████████
W.B. Colson, Thesis Advisor

███████████████
R.L. Armstead, Second Reader

███████████████
W.B. Colson, Chairman
Department of Physics

ABSTRACT

A high-current, high-power X-ray Free Electron Laser (FEL) using the Stanford linear accelerator (SLAC) as an electron beam source has been proposed. Such a system will provide the scientific community with its first realistic X-ray laser. One dramatic use a hard X-ray laser light at the proposed wavelength of 1.5 Angstrom would be to image DNA base-pairs [7].

With an accelerator already in place, the major cost of developing the SLAC system would be in the manufacturing of the undulator. The cost in building an undulator is proportional to its length. This thesis uses numerical simulation to evaluate the effectiveness of an FEL klystron in order to decrease the length of the undulator with a dispersive section.

Simulations show that the quality of the electron beam injected into the undulator can greatly effect the ability of an FEL to produce coherent light, and is a factor in determining the length of an undulator needed for saturation. In the high-gain FEL (such as proposed at SLAC), a dispersive section is sensitive to energy spread and may adversely affect the gain of the system. For moderate to low energy spread, it is found that a klystron is useful in shortening the undulator length.

By examining how the strength of a klystron dispersive section affects the gain of a high-current system, we determine a critical strength above which the klystron can be detrimental. A dispersive section that is either too strong or not strong enough will result in less than optimum gain, or an increase in the required length of an undulator.

Single-mode, phase-space simulations are used to investigate the effect on electron bunching and the onset of saturation. Longitudinal multimode simulations show the resulting coherence development.

TABLE OF CONTENTS

ACKNOWLEDGEMENT

x

I. INTRODUCTION

With the present world turmoil, the political and economic structure of current nations has made it easier for the Third World nations or even small factions of terrorist organizations to obtain state-of-the-art weapons. The advances in technology as well as hardening of modern day missiles has driven present day ship self-defense systems obsolete. The time required to track, engage, and ensure destruction of incoming weapons has decreased to seconds. Present day defense systems can no longer protect ships adequately.

The present day ship self-defense system is a layered system that relies on long and medium range missiles for long distance engagements. A ship's gun and short range missiles such as RAM and SEA SPARROW are for missiles that get through the long range defenses and are at a medium range. The final and most crucial system in the layered defense is the Phalanx Close-In-Weapon System (CIWS), for close in missiles threats. All of these systems except for CIWS, are not always available to every platform. Even if the outer defense systems are available, the detection and engagement of these incoming missiles at long ranges have become difficult with the design of sea skimming and low, slow flying missiles. The present self-defense systems must also overcome a large scale attack with multiple weapons being fired upon them simultaneously. A ship's ability to protect itself against such an attack is at present unrealistic.

CIWS has a reliable detection range of about 5000 m and an effective engagement range of less than 2000 m. A typical missile requires numerous hits from CIWS before it is destroyed. With the missiles traveling at speeds up to and greater than mach 3, the range that CIWS actually kills the missile is much closer than the 2000 m engagement range. Typically, the actual kill range is around 600 m. If CIWS is able to destroy the missile, fragments from the missile are still large enough and traveling with enough momentum to reach the ship and create significant damage. If the incoming missile is designed to maneuver once it is in close range of its target, a CIWS would have to slew its gun barrels causing the rounds to be off target until the missile stabilizes and the CIWS is locked on again. The time that a CIWS round travels to reach the incoming missile also adds to the decreasing range problem. It is evident the technology of missiles has outgrown ships' self-defense systems.

1

There is need for a speed-of-light weapon which can reach farther than CIWS and kill an incoming missile faster, so as to allow for multiple threat engagements. To kill an incoming missile with a laser, the power required on the surface of the missile is dictated by the Fluence, $F = P\Delta t/A$ [1]. Fluence (in J/cm^2), is the common measure of "hardness" of a missile. It describes the amount of energy absorbed by the missile's skin. A moderately hardened missile might require a fluence of 10 kJ/cm^2 [1]. A spot size $A = 5.0\ cm^2$ is achieved at a range $R = 5.0$ km, wavelength $\lambda = 3.8\ micron$, with a laser aperture of $D = 1.5$ meters, where

$$A = \frac{\pi R^2 \lambda^2}{D^2}\ [1].\tag{1.1}$$

P is the power received at the missile and Δt is the dwell time required to kill the missile. For a 0.1 second dwell time, the total power to destroy the missile is approximately $P = 500$ kW. The ship's weapon must emit greater power than this to overcome aerosols at sea level over the distance it travels. The power transmitted through the atmosphere decreases exponentially as $P(z) = P_0 e^{-\alpha z}$, where $\alpha = 5 \times 10^{-2}\ km^{-1}$ is the extinction coefficient for a wavelength of $\lambda = 3.8$ microns, P_0 is the initial power at the source, and z is the range to the target. At a range of 20 km the power required at the source is about 1.4 MW or greater. This amount of power has been achieved with chemical lasers. The minimal amount of time, ranging from microseconds to seconds, that the missile will travel while the laser is locked on, greatly decreases the closing distance the missile travels to only meters. This is a significant difference compared to the distance the missile closes in on its target before a CIWS obtains a kill, and it is performed at a range that is much greater than the engagement range of CIWS. The laser's speed to target also helps to reduce the closure distance. The range at which the missile is hit, even if not destroyed but damaged, is sufficient to prevent the incoming weapon from ever reaching it's target.

A Free Electron Laser (FEL) has many advantages over conventional lasers in producing high power outputs. Conventional lasers of sufficient power use dangerous chemicals that are difficult to store and are partially depleted with every firing of the laser. The depletion of the source for lasing then limits the number of times you can fire, and the number of incoming missiles that can be engaged. An FEL's power source is the electrical power from the ship, which is degraded only if the ship is already badly damaged. The FEL is tunable over a wide band of frequencies. That allows you to compensate for atmospheric conditions and concentrate the light spot on

2

the inbound missile.

The Free Electron Laser has other significant uses that can be exploited by the military, other than ship's self-defense. There are many uses in medicine such as DNA mapping and X-rays. Target tracking and identifying can be enhanced with a tunable laser. Ideally, the burden of research and development can be shared by civilian and military ensuring continuous upgrading and off-the-shelf products.

II. BACKGROUND

A. FEL THEORY

There are two major requirements for a FEL to produce emission; a relativistic electron beam supplied by an accelerator, and an undulator with a spatial periodic magnetic field [2]. The FEL creates coherent, monochromatic light by accelerating relativistic electrons in the transverse direction. The periodic magnetic field from the undulator exerts a force on the relativistic electron beam as it passes through the undulator causing the electrons to "wiggle" in the transverse direction. The electrons are accelerated from side to side causing them to spontaneously emit light in a forward cone along the electron beam axis. To collect a fraction of the spontaneously radiated electromagnetic field, mirrors are placed on the beam axis beyond both ends of the undulator creating an optical cavity. The coupling created by passing the electron beam through the stored electromagnetic field causes stimulated emission. As a result, the optical field grows and coherent light is produced from the FEL [2].

The electrons are traveling relativistically with energy γmc^2 prior to entering the undulator, where m is the electron rest mass and c is the velocity of light. The Lorentz factor of the electron is $\gamma = 1/\sqrt{1-\beta^2}$, where $\beta = v/c$ and v is the magnitude of the electron velocity. Upon entering the undulator, a force from the magnetic field acts upon the electrons causing the electrons to move back and forth in the transverse direction.

The optical field properties can be controlled by controlling the parameters of the undulator. An undulator can be of different designs using either permanent magnets or electromagnets with either linearly or circularly polarized magnetic fields producing linearly or circularly polarized light. The strength of the magnetic field determines the magnitude of deflection of the electrons and therefore the electron z velocity. Varying the electron z velocity (i.e. varying the electron energy) makes an FEL tunable over a large range of wavelengths. The undulator parameter, $K = eB\lambda_0/2\pi mc^2$, where B is the root-mean-square (rms) value of the undulator magnetic field, characterizes the undulator's magnetic field strength. In a linear undulator $B = B/\sqrt{2}$, because of non-constant acceleration, while in a helical undulator $B = B$, because of the continuous acceleration, where B is the peak magnitude of the undulator magnetic field.

5

While the quantum mechanical approach shows that the emission of a photon causes a recoil in the electron, a classical approach to the FEL theory neglecting recoil can be used because the energy loss is small. The ratio of energy lost with electron initial energy is on the order of 10^{-7}. It requires many such emissions to create an effect that would be significant, due to the high energy of the electrons. With the optical beam, the photon density is so great that the statistical fluctuations of the optical beam can also be ignored [11].

The classical approach describes an electron wiggling and emitting light while transversing the undulator's magnetic fields. The light is emitted along the electron beam axis into a forward cone. Figure 2.1 [4] shows the interaction between electrons and the optical field. It shows that the optical electric field acting on an electron will take energy away from an electron. To accomplish this transfer of energy the optical field and the electron must have the correct relative phase. The spread of electron phases in comparison to the optical field causes some of the electrons to take energy from the optical field when they are out of phase. The electrons then form bunches over the optical wavelength. The end result is that coherent light is formed from these electron bunches.

As mentioned, unlike classical lasers where coherent light is produced by electrons transitioning from one quantum state to another, the FEL produces light by the interaction of a relativistic electron beam and external forces. The FEL is then able to generate coherent light at tunable frequencies depending on the undulator parameter K. As the electrons are relativistic the undulator wavelength λ_0 is Lorentz contracted to $\lambda_0' = \lambda_0/\gamma$ in the electron beam frame. The optical field passing over the electrons is Doppler shifted to a wavelength $\lambda' = (1 + \beta_z)\gamma\lambda \approx 2\gamma\lambda$, where λ is the optical field wavelength in the lab frame [3]. To have sufficient energy exchange between the electron and the optical field a condition of resonance must occur, $\lambda' = \lambda_0'$ in the beam frame. In the undulator frame

$$\lambda = \frac{\lambda_0(1 + K^2)}{2\gamma^2} \ . \qquad (2.1)$$

By evaluating Eq. 2.1, it is apparent that an FEL can be continuously tuned by changing either the electron energy γmc^2, the undulator's magnetic field strength B, or the undulators wavelength λ_0. The undulator can also be designed to compensate for the falling out of resonance by the electrons while they give up energy. By changing
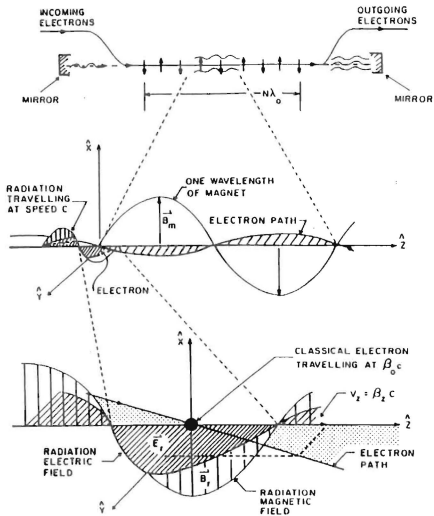
6

Figure 2-1. Fundamental physics of the FEL interaction.

λ_0 through the undulator the electron can be kept in phase with the optical field longer. This is called tapering the undulator, which increases the efficiency of the FEL.

B. ELECTRON DYNAMICS AND THE PENDULUM EQUATION

The individual electron's motion inside an undulator is described by solving the classical equations of motion. The Lorentz force is the only significant force acting on an electron traveling down the length of the undulator [3]. In the presence of the undulator and optical fields, the Lorentz force equations are

$$\frac{d(\gamma \vec{\beta})}{dt} = \frac{-e}{mc} \left[\vec{E}_r + \vec{\beta} \times (\vec{B}_r + \vec{B}_u) \right] \tag{2.1a}$$

$$\frac{d\gamma}{dt} = \frac{-e}{mc} (\vec{\beta} \cdot \vec{E}_r) \tag{2.1b}$$

$$\gamma^{-2} = 1 - (\vec{\beta} \cdot \vec{\beta}) \quad , \tag{2.1c}$$

where $\vec{\beta} = \vec{v}/c$ is the electron normalized velocity vector. The magnetic field of a helical undulator $\vec{B}_u$ is circularly polarized and is given by

$$\vec{B}_u = B \left[cos(k_0 z), \, sin(k_0 z), \, 0 \right] \quad , \tag{2.2}$$

where the undulator wave number $k_0 = 2\pi/\lambda_0$, and z is the direction of the undulator axis. The optical electric and magnetic fields are assumed to be circularly-polarized plane waves and are given by

$$\vec{E}_r = E \left[cos(\psi), \, -sin(\psi), \, 0 \right] \quad , \quad \vec{B}_r = E \left[sin(\psi), \, cos(\psi), \, 0 \right] \quad , \tag{2.3}$$

where E is the optical field magnitude and $\psi = kz + \omega t + \phi$. The optical wave number is $k = 2\pi/\lambda$, the optical frequency is $\omega = ck$, and ϕ is the phase of the optical wave.

Substituting the undulator magnetic field Eq. 2.2 and the optical wave electromagnetic fields Eq. 2.3 into the Lorentz force equations Eq. 2.1 , they become:

$$\frac{d}{dt} (\gamma \vec{\beta}_\perp) = \frac{-e}{mc} \left[E(2 - \beta_z)(cos(\psi), -sin(\psi), 0) + \beta_z \, B(-sin(k_0 z), \, cos(k_0 z), 0) \right] \tag{2.4a}$$

$$\frac{d}{dt} (\gamma \vec{\beta}_z) = \frac{-e}{mc} \left[E(\beta_x cos(\psi) - \beta_y sin(\psi)) + B(\beta_x sin(k_0 z), - \beta_y cos(k_0 z)) \right] \tag{2.4b}$$

$$\frac{d\gamma}{dt} = -\frac{e}{mc} E \left[\beta_x cos(\psi) - \beta_y sin(\psi) \right] \quad , \tag{2.4c}$$

where $\vec{\beta}_\perp = (\beta_x, \beta_y, 0)$. As the electrons travel down the undulator in the z direction

they are acted upon by a transverse force from the optical electric and magnetic fields and the magnetic field from the undulator. The force from the optical field is proportional to $E\,(1-\beta_z)$ while the force from the undulator magnetic field is proportional to $\beta_z\,B$. For a relativistic electron $\beta_z \rightarrow 1$, so $1-\beta_z \rightarrow 0$. Therefore, we can assume $E\,(1-\beta_z) \ll B\,\beta_z$. The force acting on the electron in the transverse direction is mainly due to the undulator magnetic field. Equation 2.4a can then be approximated as

$$\frac{d}{dt}(\gamma\vec{\beta}_\perp) = \frac{-e}{mc}\,\beta_z\,B[-sin(k_0 z),\,cos(k_0 z),\,0]\quad. \tag{2.5}$$

On integrating Eq. 2.5, the electron's velocity in the transverse direction is found to be

$$\vec{\beta}_\perp = -\frac{K}{\gamma}[cos(k_0 z),\,sin(k_0 z),\,0]\quad, \tag{2.6}$$

where $K = eB\lambda_0/2\pi mc^2 = eB/k_0 mc^2$ is the undulator parameter.

Examining the transverse and longitudinal motion of the electron as it travels down the undulator, it is noted that the transverse motion is small, $\beta_\perp \approx K/\gamma \ll 1$.

Inserting Eq. 2.7 into Eq. 2.5c gives the electron energy evolution,

$$\frac{d\gamma}{dt} = \dot{\gamma} = -\frac{e}{mc}(\vec{\beta}_\perp \cdot \vec{E}_r) = \frac{eKE}{\gamma mc}cos(\zeta + \phi)\quad, \tag{2.7}$$

where the dimensionless electron phase in the combined undulator and optical fields is $\zeta + \phi = \psi + k_0 z = (k + k_0)z - \omega t + \phi$. The initial value of the electron phase is $\zeta(0) = \zeta_0 = (k + k_0)z_0$. Since $k \gg k_0$ then $\zeta_0 \approx kz_0 = 2\pi z_0/\lambda$, when $\gamma \gg 1$. The electron phase ζ determines the electron's z position relative to a single optical wavelength λ. By using Eq. 2.1c and inserting $\vec{\beta}_\perp$ in Eq. 2.6 gives

$$\gamma^{-2} = 1 - \beta_z^2 - \beta_\perp^2 = 1 - \beta_z^2 - \frac{K^2}{\gamma^2}\quad, \tag{2.8}$$

or

$$(1 + K^2)\gamma^{-2} = 1 - \beta_z^2\quad. \tag{2.9}$$

Then, take the time derivative of both sides

$$-2\gamma^{-3}\dot{\gamma}\,(1 + K^2) = -2\beta_z\dot{\beta}_z\quad, \tag{2.10}$$

which relates $\dot{\gamma}$ to $\dot{\beta}_z$ as

$$\frac{\dot{\gamma}}{\gamma} = \frac{\gamma^2\beta_z\dot{\beta}_z}{(1 + K^2)}\quad. \tag{2.11}$$

9

Taking the first derivative of the electron phase ζ gives

$$\dot{\zeta} = (k + k_0)\dot{z} - \omega = (k + k_0)c\beta_z - \omega \quad , \tag{2.12}$$

and a second derivative gives

$$\ddot{\zeta} = (k + k_0)c\dot{\beta}_z \quad . \tag{2.13}$$

By using Eq. 2.11, and Eq. 2.13, and the resonance condition

$$\frac{\dot{\gamma}}{\gamma} = \frac{\gamma^2\beta_z\ddot{\zeta}}{(1 + K^2)(k + k_0)} \propto \frac{\gamma^2\ddot{\zeta}}{\omega(1 + K^2)} \propto \frac{\ddot{\zeta}}{2\omega_0} \quad , \tag{2.14}$$

where $\omega_0 = \omega(1 + K^2)/2\gamma^2$. The electron's equation of motion Eq. 2.7 can be combined with Eq. 2.14 to give

$$\ddot{\zeta} = \frac{2\omega_0 eKE}{\gamma^2 mc} \cos(\zeta + \phi) \quad . \tag{2.15}$$

Define the dimensionless time $\tau = ct/L$ where L is the length of the undulator to make the equation of motion, Eq. 2.15, dimensionless. As an electron passes through the undulator, $\tau = 0 \rightarrow 1$. The dimensionless optical field is defined as $a = |a|e^{i\phi}$, where $|a| = 4\pi NeKLE/\gamma^2mc^2$, and N is the number of periods in the undulator. The pendulum equation can be written as

$$\overset{\circ\circ}{\zeta} = \overset{\circ}{v} = |a| \cos(\zeta + \phi) \quad , \tag{2.16}$$

where $\overset{\circ\circ}{\zeta}$ is the second derivative with respect to τ, $\overset{\circ}{v}$ is the first derivative with respect to τ, and the dimensionless electron phase velocity is defined as $v = L [(k + k_0)\beta_z - k]$. When $v = 0$, the electrons are at resonance with the optical wave and $\lambda = \lambda_0(1 + K^2/2\gamma^2)$. Changes in the electrons' energy correspond to giving or taking energy from the optical wave. As the electron decreases its energy, its phase velocity decreases and it gives up energy to the optical wave. The maximum energy loss of the electron occurs when $\zeta + \phi = \pi$.

C. THE FREE ELECTRON LASER WAVE EQUATION

The development of a complex optical wave equation starts from Maxwell's wave equation acting on a vector potential $\vec{A}(r,t)$ driven by the current density $\vec{J}_\perp$,

$$\left[\vec{\nabla}^2 - \frac{1}{c^2}\frac{\partial^2}{\partial t^2} \right] \vec{A}(z,t) = -\frac{4\pi}{c} \vec{J}_\perp \quad , \tag{2.17}$$

10

where $\vec{\nabla}^2 = \partial^2/\partial x^2 + \partial^2/\partial y^2 + \partial^2/\partial z^2$, the vector potential $\vec{A}(z,t)$ is

$$\vec{A}(z,t) = \frac{c}{\omega} E(z,t) \left[\sin(kz - \omega t + \phi(z,t)), \cos(kz - \omega t + \phi(z,t)), 0 \right] , \qquad (2.18)$$

and the electric field $\vec{E}$ is

$$\vec{E} = E(z,t)[\cos(kz - \omega t + \phi(z,t)), -\sin(kz - \omega t + \phi(z,t)), 0] , \qquad (2.19)$$

where

$$\vec{E} = -\frac{1}{c} \frac{\partial \vec{A}}{\partial t} . \qquad (2.20)$$

Since the wave is traveling only in the z direction the Maxwell wave equation operator then is

$$\frac{\partial^2}{\partial z^2} - \frac{1}{c^2} \frac{\partial^2}{\partial t^2} . \qquad (2.21)$$

Taking the first derivative of the vector potential $\vec{A}$ with respect to z gives

$$\frac{\partial \vec{A}}{\partial z} = \frac{1}{k} \frac{\partial E}{\partial z} [\sin(\psi), \cos(\psi), 0] + \frac{E}{k} \left(k + \frac{\partial \phi}{\partial z} \right) [\cos(\psi), -\sin(\psi), 0] , \qquad (2.22)$$

where $\psi = kz - \omega t + \phi$, and $c/\omega = 1/k$. Taking the second derivative with respect to z gives

$$\frac{\partial^2 \vec{A}}{\partial z^2} = \frac{1}{k} \frac{\partial E}{\partial z} \left[k + \frac{\partial \phi}{\partial z} \right] [\cos(\psi), -\sin(\psi), 0]$$

$$+ \frac{1}{k} \frac{\partial^2 E}{\partial z^2} [\sin(\psi), \cos(\psi), 0] + \frac{1}{k} \frac{\partial E}{\partial z} \left[k + \frac{\partial \phi}{\partial z} \right] [\cos(\psi), -\sin(\psi), 0]$$

$$+ \frac{E}{k} \frac{\partial^2 \phi}{\partial z^2} [\cos(\psi), -\sin(\psi), 0] + \frac{E}{k} (k + \frac{\partial \phi}{\partial z})^2 [-\sin(\psi), -\cos(\psi), 0] . \qquad (2.23)$$

Assuming slowly varying amplitudes and phases where $\partial E/\partial z \ll kE$, $\partial \phi/\partial z \ll k\phi$, $\partial E/\partial t \ll \omega E$, $\partial \phi/\partial t \ll \omega\phi$, and $\omega = kc$ allows us to use only first-order terms and simplify Eq. (2.23) to

$$\frac{\partial^2 \vec{A}}{\partial z^2} \approx 2 \frac{\partial E}{\partial z} [\cos(\psi), -\sin(\psi), 0] + \frac{E}{k} \left(k + \frac{\partial \phi}{\partial z} \right)^2 [-\sin(\psi), -\cos(\psi), 0] . \qquad (2.24)$$

By expanding

$$\left[k + \frac{\partial \phi}{\partial z} \right]^2 = k^2 + 2 k \frac{\partial \phi}{\partial z} + \left(\frac{\partial \phi}{\partial z} \right)^2 , \qquad (2.25)$$

11

knowing $(\partial\phi/\partial z)^2 \ll \partial\phi/\partial z$, and putting Eq. 2.25 into Eq. 2.24, it becomes

$$\frac{\partial^2 \vec{A}}{\partial z^2} \approx 2 \; \frac{\partial E}{\partial z} \; [\cos(\psi), \; -\sin(\psi), \; 0] + \left[k \; E + 2 \; E \; \frac{\partial \phi}{\partial z} \right] [-\sin(\psi), \; -\cos(\psi), \; 0] \quad . \tag{2.26}$$

The time derivative portion of the Maxwell's wave equation operator is

$$\frac{1}{c^2} \; \frac{\partial^2 \vec{A}}{\partial t^2} = \frac{1}{c^2} \; \frac{\partial^2}{\partial t^2} \; \frac{c}{\omega} \; E \; [\sin(\psi), \; \cos(\psi), \; 0] \quad . \tag{2.27}$$

Taking the first derivative with respect to time gives

$$\frac{\partial}{\partial t} \; [E \; (\sin(\psi), \; \cos(\psi), \; 0)] = \frac{\partial E}{\partial t} [\sin(\psi), \; \cos(\psi), \; 0]$$

$$+ E \left[\frac{\partial \phi}{\partial t} - \omega \right] [\cos(\psi), \; -\sin(\psi), \; 0] \quad . \tag{2.28}$$

The second derivative gives

$$\frac{\partial^2 E}{\partial t^2} [\sin(\psi), \; \cos(\psi), \; 0] = \frac{\partial E}{\partial t} \left[\frac{\partial \phi}{\partial t} - \omega \right] \cos(\psi), \; -\sin(\psi), \; 0] + \frac{\partial^2 E}{\partial t^2} [\sin(\psi), \; \cos(\psi), \; 0]$$

$$+ \frac{\partial E}{\partial t} \left[\frac{\partial \phi}{\partial t} - \omega \right] [\cos(\psi), \; -\sin(\psi), \; 0] + E \frac{\partial^2 \phi}{\partial t^2} [\cos(\psi), \; -\sin(\psi), \; 0]$$

$$+ E \left[\frac{\partial \phi}{\partial t} - \omega \right]^2 [-\sin(\psi), \; -\cos(\psi), \; 0] \quad . \tag{2.29}$$

Again, assuming the slowly varying amplitudes and phases allows us to neglect all but first-order terms, so Eq. 2.29 becomes

$$\frac{\partial^2 \vec{A}}{\partial t^2} \approx -2 \; c \; \frac{\partial E}{\partial t} [\cos(\psi), \; -\sin(\psi), \; 0] + \frac{c}{\omega} \; E \left[\frac{\partial \phi}{\partial t} - \omega \right]^2 [-\sin(\psi), \; -\cos(\psi), \; 0] \tag{2.30}$$

By expanding

$$\left[\frac{\partial \phi}{\partial t} - \omega \right]^2 = \left[\frac{\partial \phi}{\partial t} \right]^2 - 2 \; \omega \; \frac{\partial \phi}{\partial t} + \omega^2 \quad , \tag{2.31}$$

again knowing $(\partial\phi/\partial t)^2 \ll \partial\phi/\partial t$, we put Eq. 2.31 into Eq. 2.30 and it becomes

$$\frac{\partial^2 \vec{A}}{\partial t^2} \approx -2 \; c \; \frac{\partial E}{\partial t} [\cos(\psi), \; -\sin(\psi), \; 0] + c \; (\omega \; E - 2 \; E \; \frac{\partial \phi}{\partial t}) [-\sin(\psi), \; -\cos(\psi), \; 0] \tag{2.32}$$

Putting Eq. 2.26 and Eq. 2.32 into Eq. 2.17 gives

$$\left[\frac{\partial^2}{\partial z^2} - \frac{1}{c^2} \frac{\partial^2}{\partial t^2} \right] \vec{A} = 2 \left[\frac{\partial E}{\partial z} + \frac{1}{c} \frac{\partial E}{\partial t} \right] \vec{e}_1 + 2 E \left[\frac{\partial \phi}{\partial z} + \frac{1}{c} \frac{\partial \phi}{\partial t} \right] \vec{e}_2 \quad , \quad (2.33a)$$

where the unit vectors are $\vec{e}_1 = [\cos(\psi), \sin(\psi), 0]$ and $\vec{e}_2 = [-\sin(\psi), -\cos(\psi), 0]$. We also know Eq. 2.33a is a multiple of the current density in Eq. 2.17 so

$$- \frac{4\pi}{c} \vec{J}_\perp = 2 \left[\frac{\partial E}{\partial z} + \frac{1}{c} \frac{\partial E}{\partial t} \right] \vec{e}_1 + 2 E \left[\frac{\partial \phi}{\partial z} + \frac{1}{c} \frac{\partial \phi}{\partial t} \right] \vec{e}_2 \quad . \quad (2.33b)$$

To solve for the time variation of the field envelope make the change of variables $z \to z - c\,t$. Then $\bar{z} = z + c\,t$ where the undulator length $L = N\lambda_0$, N is the number of periods, λ_0 is the wavelength of the undulator, and $\tau = ct/L$ is the dimensionless time. By making the change of variables, we change the partial derivatives,

$$\frac{\partial}{\partial z} = \frac{\partial \bar{z}}{\partial z} \frac{\partial}{\partial \bar{z}} + \frac{\partial \tau}{\partial z} \frac{\partial}{\partial \tau} = 1 \frac{\partial}{\partial \bar{z}} + 0 \quad , \quad (2.34)$$

and

$$\frac{1}{c} \frac{\partial}{\partial t} = \frac{1}{c} \frac{\partial \bar{z}}{\partial t} \frac{\partial}{\partial \bar{z}} + \frac{1}{c} \frac{\partial \tau}{\partial t} \frac{\partial}{\partial \tau} = - \frac{\partial}{\partial \bar{z}} + \frac{1}{L} \frac{\partial}{\partial \tau} \quad . \quad (2.35)$$

Putting Eq. 2.34 and Eq. 2.35 together simplifies the differential operator to

$$\frac{\partial}{\partial z} + \frac{1}{c} \frac{\partial}{\partial t} = \frac{1}{L} \frac{\partial}{\partial \tau} \quad . \quad (2.36)$$

Making the substitution Eq. 2.36 into Eq. 2.33b and projecting onto $\vec{e}_1$ gives

$$- \frac{4\pi}{c} \vec{J}_\perp \cdot \vec{e}_1 = 2 \frac{1}{L} \frac{\partial E}{\partial \tau} \quad . \quad (2.37)$$

Doing the same to Eq. 2.33b but projecting onto $\vec{e}_2$ gives

$$- \frac{4\pi}{c} \vec{J}_\perp \cdot \vec{e}_2 = 2 E \frac{1}{L} \frac{\partial \phi}{\partial \tau} \quad . \quad (2.38)$$

The current density for a single electron is $\vec{J}_\perp = - ec\vec{\beta}_\perp$. The electron trajectory will be found to be $\vec{\beta}_\perp = - (K/\gamma) [\cos(k_0 z), \sin(k_0 z), 0]$, so that

$$\vec{J}_\perp = \frac{ecK}{\gamma} [\cos(k_0 z), \sin(k_0 z), 0] \quad , \quad (2.39)$$

where $\gamma = 1/\sqrt{1 - v^2/c^2}$, v is the velocity of the electron, k_0 is the undulator wave number $2\pi/\lambda_0$, and the undulator parameter is $K = eB/mk_0 c$.

Inserting Eq. 2.39 and the value for $\vec{\varepsilon}_1$ into Eq. 2.37 gives

$$\frac{\partial E}{\partial \tau} = -\frac{2\pi L e K}{\gamma} [\cos(k_0 z), \sin(k_0 z), 0] \cdot [\cos(\psi), \sin(\psi), 0] \quad . \tag{2.40}$$

On performing the dot product, Eq. 2.40 becomes

$$\frac{\partial E}{\partial \tau} = -\frac{2\pi L e K}{\gamma} \cos(\zeta + \phi) \quad , \tag{2.41}$$

where the electron phase is $\zeta = (k + k_0)z - \omega t$.

The wave equation Eq. 2.41 is for a single electron. The average value over many electrons gives

$$\frac{\partial E}{\partial \tau} = -\frac{2\pi L e K \rho}{\gamma} <\cos(\zeta + \phi)> \quad , \tag{2.42}$$

where ρ is the electron particle density and

$$<\cos(\zeta + \phi)> = \sum_{i=0}^{N_e} \frac{\cos(\zeta_i + \phi_i)}{N_e} \quad . \tag{2.43}$$

Similar manipulations of Eq. 2.38 gives us

$$\frac{\partial \phi}{\partial \tau} = -\frac{2\pi L e K \rho}{\gamma} <\sin(\zeta + \phi)> \quad . \tag{2.44}$$

The complex electric field is $E = |E| \, e^{i\,\phi}$ so

$$\frac{\partial E}{\partial \tau} = \frac{\partial |E|}{\partial \tau} e^{i\,\phi} + i \, |E| \, \frac{\partial \phi}{\partial \tau} e^{i\,\phi} \quad . \tag{2.45}$$

When Eq. 2.42 and Eq. 2.44 are inserted into Eq. 2.45, we get

$$\frac{\partial E}{\partial \tau} = -\frac{2\pi L e K \rho}{\gamma} [<\cos(\zeta + \phi)> - i <\sin(\zeta + \phi)>] \, e^{i\,\phi} \quad , \tag{2.46}$$

which is also

$$\frac{\partial E}{\partial \tau} = -\frac{2\pi L e K \rho}{\gamma} <e^{-i\,(\zeta + \phi)}> e^{i\,\phi} \quad . \tag{2.47}$$

From the pendulum equation, we know that our dimensionless optical wave field is $a = |a| \, e^{i\,\phi}$, where $|a| = 4\pi N K L e |E| / \gamma^2 mc^2$, so that

$$\frac{\partial a}{\partial \tau} = \overset{\circ}{a} = -\frac{8\pi^2 e^2 \rho N K^2 L^2}{\gamma^3 mc^2} <e^{-i\,(\zeta + \phi)}> e^{i\,\phi} \quad . \tag{2.48}$$

The dimensionless current is $j = 8\pi^2 e^2 \rho N K^2 L^2 / \gamma^3 m c^2$. Which leads us to the Free Electron Laser optical wave equation

$$\overset{\circ}{a} = -j <e^{-i\,\zeta}> \quad . \tag{2.49}$$

Looking at the real and imaginary parts of Eq. 2.49, you have

$$|\overset{\circ}{a}| = -j <\cos(\zeta + \phi)>, \quad \overset{\circ}{\phi} = \frac{j}{|a|} <\sin(\zeta + \phi)> \quad , \tag{2.50}$$

where $|a|$ is the optical field amplitude and ϕ is the optical field phase. Equation Eq. 2.50 shows that bunching of electrons in phase at $(\zeta + \phi) = \pi$ drives the optical wave amplitude and produces a gain, while bunching electrons around $(\zeta + \phi) = \pi/2$ will drive the optical phase. Increasing the electron beam current density j will increase gain and optical phase evolution. The optical fields increase in magnitude will reduce the effects of the electron phase evolution.

D. LOW GAIN FEL

The Maxwell-Lorentz (standard classical, i.e. non-quantum dynamics) theory for an FEL can be formed by combining the simple pendulum equation, Eq. 2.16, and the optical wave equation, Eq. 2.49. The strength of the dimensionless current density j governs the coupling between electrons and light. It determines the response of the optical wave to the bunching of electrons in phase ζ. The Maxwell-Lorentz theory is generally valid for both weak ($|a| \ll \pi$) or strong ($|a| \gg \pi$) optical fields [5].

From the pendulum equation, Eq. 2.16, it is evident that the electron energy loss is greatest when the electron bunch is at $\zeta + \phi = \pi$, which provides for the maximum gain in the optical field. As the electron bunch moves toward $\zeta + \phi = 0$, over-bunching occurs and energy is absorbed back into the electron beam.

Maximum coupling between the optical field and the electron beam occurs when the initial electron phase velocity is at resonance, $\nu_0 = 0$ [6]. A "realistic" beam of monoenergetic electrons will enter the undulator with a random spread in phase ζ. There will be just as many electrons gaining energy from, as losing energy to, the optical field, resulting in zero gain. To achieve a useful gain, the electrons must have a velocity slightly above resonance so that more electrons give up energy than absorb it in an exchange with the optical field.

To understand the operation of an FEL, it is useful to examine the evolution of the electrons as they move through phase space (ζ, ν). The path in phase space for each electron is dependent on the initial values of ζ_0 and ν_0. A low-gain FEL produces an electron phase-space path that can be represented by a simple mechanical pendulum [3], and is shown analytically by

$$\nu^2 = \nu_0^2 - 2 |a| [\sin(\zeta + \phi) - \sin(\zeta_0)] \quad . \tag{2.51}$$

By examining Eq. 2.51, we can note that there are fixed points, $(\pi/2, 0)$ and $(3\pi/2, 0)$, where the pendulum does not evolve. The electrons near these phase space points evolve slowly. The electrons that are at the stable fixed point $(\pi/2, 0)$ correspond to a pendulum at the bottom of its arc. The electrons with a large phase velocity $|\nu| > 2|a|^{1/2}$ are in an open orbit. This would correspond to a pendulum swinging in one direction continuously about its pivot point. An electron in a closed orbit is like a pendulum swinging with a small amplitude oscillating about the stable fixed point. A change in ϕ would cause a change in the horizontal position of the pendulums fulcrum. The phase-space path that separates the open and closed orbits of an electron is called the "separatrix" and is given by

$$\nu_s^2 = 2 |a| [1 - \sin(\zeta_s + \phi)] \quad . \tag{2.52}$$

The separatrix has a peak-to-peak height of $4|a|^{1/2}$. Its horizontal position depends on the optical phase ϕ. As the optical field grows, so does the separatrix height.

Since the electron's evolution in phase space is periodic over each optical wavelength λ, the interaction in an FEL can be modeled by tracking sample electrons over one wavelength. Figure 2-2 is an example of a phase space plot with low current $j = 1$, a moderate optical field strength of $|a| = 4$, and an electron phase velocity of $\nu_0 = 2.6$.

The electrons enter the undulator at $\tau = 0$, in a uniform distribution of initial phases, $\zeta_0 = -\pi/2 \to 3\pi/2$. The electrons then interact with the optical field of strength $a_0 = 4$. The initial electrons are displayed as light gray dots. As they evolve through the undulator they become darker until they become black dots at the end of the undulator, $\tau = 1$. The electrons to the left experience an increase in phase velocity which causes them to move to the right, while the electrons to the right experience a loss of energy and decrease in phase velocity. This produces a spatial bunching observed near phase $\zeta = \pi$ at $\tau = 1$, so more electrons are giving up energy than taking energy away from the optical field. There is a limit in the process of energy
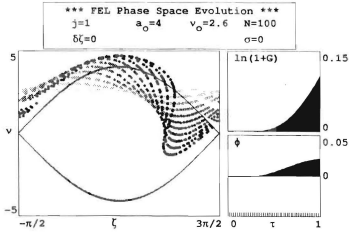
16

Figure 2-2. Phase-space plot for electrons entering with $\nu_0 = 2.6$.

exchange where the electrons have given up so much energy that their phase and phase velocity cause the electrons to start absorbing energy back from the optical field. An undulator's length can be designed to prevent the electrons from reaching this stage.

The optical gain is defined as the fractional increase in optical field power over time τ,

$$G(\tau) = \frac{(a(\tau)^2 - a_0^2)}{a_0^2} \quad . \tag{2.53}$$

Gain is pictorially displayed in the upper right graph of the phase space Figure 2-2. The electrons in the beam are assumed to be uniformly distributed in phase ζ_0 and have the same initial phase velocity ν_0. A change in electron energy corresponds to a change in electron phase velocity. The average energy lost by an electron is $\gamma mc^2(\langle \nu \rangle - \nu_0)/4\pi N$. The energy lost by the electron determines the optical gain to be $G = 2j(\nu_0 - \langle \nu \rangle)/a_0^2$ [3]. The phase velocity average is found by expanding the pendulum equation, Eq. 2.16. The small signal gain equation becomes [3]

$$G(\tau) = j\left[\frac{2 - 2\cos(\nu_0\tau) - \nu_0\tau \sin(\nu_0\tau)}{\nu_0^3}\right] \quad . \tag{2.54}$$

17

If the phase velocity is far away from resonance, $|v_0| \gg \pi$, the final gain at $\tau = 1$ will be small. Optimum coupling, resulting in maximum gain, occurs when $|v_0| \lesssim \pi$. The natural gain bandwidth for an FEL is derived from the relation $\Delta v_0 \approx 4\pi N \Delta \gamma / \gamma$. The natural gain bandwidth is

$$\left| \frac{\Delta \gamma}{\gamma} \right| \approx \frac{1}{2N} \quad . \tag{2.55}$$

An FEL gain spectrum and optical phase shift is plotted in Figure 2-3, for a weak field $a_0 = 1$, low current $j = 1$, and the initial phase velocity between the interval $-12 \leq v_0 \leq 12$. The gain curve is antisymmetric about v_0 with maximum gain at $v_0 = 2.6$.
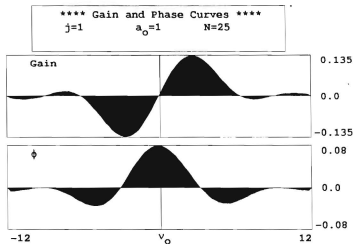
Figure 2-3. Weak-field, low-gain FEL gain spectrum and optical phase shift plot.

E. ENERGY SPREAD

The previous section dealt with a perfect beam where the electrons were uniformly distributed over the optical wavelength with the same initial energy. This is not achievable, since there is a trade-off between electron beam quality and current density. Increasing current I tends to decrease beam quality from the accelerator, while increasing the length of the undulator by increasing N increases the FEL's sensitivity to beam quality because the natural gain bandwidth is narrower. Where the natural gain bandwidth is defined as the range of phase velocities where the growth rate is reduced by 10 % below its peak value [3].

There are two qualities that describe electron beam quality: the electron beam energy spread, $\Delta\gamma/\gamma$, and emittance, ε. Electrons with same initial phase ζ, but different phase velocities will drift apart on the z axis [6]. At the end of the undulator their final phase difference is roughly $\Delta\zeta \approx \Delta\nu\tau$, where $\tau = 1$, for each electron. It is apparent, for a change in initial energy $\Delta\gamma mc^2$, there is a corresponding change in electron phase velocity, $\Delta\nu \approx 4\pi N\Delta\gamma/\gamma$. A Gaussian distribution of energies with an rms spread , $\Delta\gamma/\gamma$, is characterized by standard deviation $\sigma_G = 4\pi N\Delta\gamma/\gamma$. When $\sigma_G \approx \pi$, bunching becomes impaired [6]. Typical energy spreads from an accelerator are on the order of $\Delta\gamma/\gamma \approx 0.001$.

Emittance, ε, is the average angular spread times the average beam radius, $\varepsilon = r\bar{\theta}$, where r is the average beam radius and $\bar{\theta}$ is the average angular divergence of the electron beam. The normalized emittance, $\varepsilon_n = \varepsilon\gamma = r\bar{\theta}\gamma$, is a measure for beam quality. As the electrons are accelerated and beam energy increases, the normalized emittance remains constant. There is a Gaussian spread in angles with rms value $\bar{\theta}$ resulting in an exponential distribution of phase velocities. The standard deviation in θ is $\sigma_\theta = 4\pi N\gamma^2\bar{\theta}^2/(1 + K^2)$. As with σ_G, when σ_θ is equal to or greater than π, electron bunching is impaired.

F. HIGH-CURRENT HIGH-GAIN FEL

In high current, high gain FELs $j \gg \pi$, the magnitude of the optical field changes significantly over a single pass of the electrons through the undulator. This is evident in the wave equation, Eq. 2.49. As we did in the low gain FEL, assume a perfect quality beam operating on resonance, $\nu_0 = 0$. From the pendulum and wave equations, the optical field grows exponentially for large j as it travels down the

19

undulator [3]:

$$|a(\tau)| \approx \frac{a_0}{3} e^{(j/2)^{1/3}\sqrt{3}\tau/2} \quad ;$$ (2.56)

and the phase evolves as:

$$\phi(\tau) \approx \left(\frac{j}{2}\right)^{1/3} \frac{\tau}{2} \quad .$$ (2.57)

The FEL gain for large j is

$$G(\tau) \approx \frac{1}{9} e^{(j/2)^{1/3}\sqrt{3}\tau/2} \quad .$$ (2.58)

For an electron beam that is off resonance, the single pass gain is

$$G(\nu_0) \approx \frac{1}{9} e^{(j/2)^{1/3}\sqrt{3}(1-(\nu_0\tau_B/3)^5)} \quad ,$$ (2.59)

where $\tau_B = (2/j)^{1/3}$ is the bunching time. The peak gain will occur slightly above resonance. The phase velocity has now become a function of current. As $j \to \infty$ the gain spectrum becomes symmetric centered at resonance.

The gain bandwidth is $\Delta\nu_0 \approx 2j^{1/3}$. The bandwidth for a low gain FEL is $\Delta\nu_0 \approx \pi/2$. It is evident that the bandwidth for the high gain case can be much larger than that for the low gain FEL.

G. THE KLYSTRON UNDULATOR

The purpose of a "dispersive section" in a klystron undulator is to increase optical gain in a weak optical field. There are three major sections to a klystron undulator. The undulator that was described earlier is divided into two sections separated by a "drift section" or a "dispersive section". The first section of the undulator is called the "modulator". It develops the phase velocity differences to prepare the electrons for bunching. The next portion is either a drift section, i.e. an open section that allows the electrons to continue their bunching without interaction with an optical field, or a dispersive section, made up of magnets that force the electrons far off resonance. The final section of the undulator is called the "radiator", where the electrons and the optical field interact and create the coherent optical beam.

Mathematically, there is no difference between the use of a drift section or a dispersive section [3]. The drift section requires a large distance over which the electrons travel with no optical interaction. This is easily achieved, but can possibly double the length of the undulator, or even larger. A dispersive section forces the electrons off centerline in an arc, and allows for the use of a shorter undulator. The strength of either type of system is given by the dimensionless drift time D, where D can be determined by the number of undulator periods equivalent to the drift space,

$$D = \frac{N_d}{N} \quad , \tag{2.60}$$

where N_d is the length of the drift space in undulator periods.

While the electrons are traveling in the modulator and radiator the equations governing their motion are still Eq. 2.16 and 2.49. While in the dispersive or drift section there is no electron-optical wave interaction. The only change in electron phase is caused by the constant phase velocity, v; therefore, the change in phase velocity is $\Delta v = 0$, so $\Delta \zeta = vD$ is the only change in electron phase. The electrons then will bunch without any interaction from the optical field, and the optical field strength will not grow.

When using a klystron the gain and phase equation are [3]

$$G(v_0) \approx \frac{jD}{4} \sin(v_0 D) \quad , \tag{2.61}$$

and

$$\phi(v_0) \approx \frac{jD}{8} \cos(v_0 D) \quad . \tag{2.62}$$

It is apparent that the maximum gain is about $jD/4$ when $v_0 = \pi/2D$. It is also apparent that with low j, the addition of a klystron enhances gain. The spread in initial phase velocity is critical. The natural gain bandwidth becomes narrower, dictating that beam quality improve. The spread in initial phase velocity should be kept to $\Delta v_0 \le \pi/D$, which is smaller than that required for a regular undulator. The stronger the dispersive section, the greater the need for increased beam quality.

Figures 2-4a and 2-4b are the optical gain spectra for a low-current ($j = 1$), weak-field ($a_0 = 1$), FEL without a klystron and with a klystron, $D = 2$. Along with the narrowing of the natural bandwidth, gain is significantly improved by addition of a drift section or dispersive section.

21

Figures 2-5a and 2-5b are the optical gain spectra for a high-current ($j = 100$), weak-field ($a_0 = 1$) FEL without a klystron and with a klystron of magnitude $D = 2$. The natural bandwidth is increased and gain is significantly improved with the use of a klystron undulator even in a high-current FEL. The size of D for a high-current FEL is significantly smaller than that for a low-current FEL.
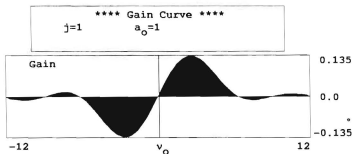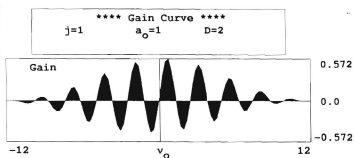

Figure 2-4a. Low-current, weak-field FEL gain spectrum, without dispersive section.

Figure 2-4b. Low-current, weak-field FEL gain spectrum, with dispersive section.
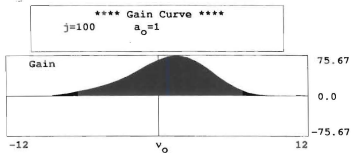
Figure 2-5a. High-current, weak-field FEL gain spectrum, without dispersive section.
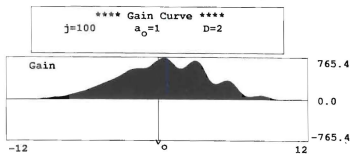
Figure 2-5b. High-current, weak-field FEL gain spectrum, with dispersive section.

III. SLAC X RAY FREE ELECTRON LASER

A. INTRODUCTION

Research in the area of high power FEL's is important to the military for the development of missile defense. The research and development that is being performed at SLAC is in the high peak power (GeV) FEL regime. By developing hard X ray laser light at a wavelength of 1.5 Å, imaging of DNA base-pairs may be accomplished [7]. The FEL is the best possible source for an X ray laser.

The SLAC project proposes to develop coherent hard X ray radiation at wavelengths as short as 1.5 Å. It will use a single pass of an electron beam through an undulator with no initial optical field. The optical field will be started from noise using a process called Self-Amplified Spontaneous Emission (SASE). There are no mirrors for feedback of the optical beam. The electron beam makes a single pass through the undulator creating a cone of light in the direction of the electron beam's path. The only interaction between the electron beam and the optical field happens during this single pass. Figure 3-1 is a diagram of the system proposed by SLAC. It combines the use of the SLAC linear accelerator (linac) with an undulator to produce the coherent X ray light. The mirror merely directs the light beam at grazing angles.
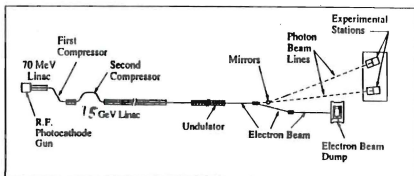

Figure 3-1. Schematic of the SLAC linac driving a coherent X ray FEL.

The system design would incorporate a section of the SLAC linac accelerating the electron beam to an energy of $\gamma mc^2 = 15$ GeV with peak current of $I = 5000$ A. Table 3-1 contains the design parameters for two systems that would produce either a

4.5 Å or 1.5 Å laser beam [8].

PARAMETERS	A	B
λ (Radiation Wavelength)	1.5 Å	4.5 Å
λ_0 (Undulator period)	2.67 cm	4.0 cm
B (Peak undulator field)	1.173 T	1.66 T
Undulator type	Helical	Linear
K Undulator parameter (peak)	3.4	4.2
γmc^2 (Electron energy)	15 GeV	15 GeV
I (Peak current)	5000 A	5000 A
$\Delta\gamma/\gamma$ (Energy spread)	0.0002	0.0002
L (Undulator length)	25 m	38 m
Output power	11 GW	66 GW

Table 3-1. Proposed parameters for an X ray FEL at SLAC.

The dimensionless current for $I = 5000$ A is $j = 2056$ for the 4.5 Å laser and $j = 3121$ for the 1.5 Å laser. As mentioned earlier, the dimensionless current determines the response of the optical wave to the electron beam bunching. The gain of the system, because of the high j, is in the high-gain regime. Figure 3-2 is a phase-space plot for the 4.5 Å system and figure 3-3 is for the 1.5 Å system. Each simulation is started from an optical field $a_0 = 0$ and the electrons are all started with random initial phase ζ between $-\pi/2$ and $3\pi/2$. The simulations ran with an undulator length of $L = 35$ m. A filling factor $F = 0.1$ was used, where the filling factor is the ratio of the area of the electron beam to the optical beam. The electron beam radius $r_b = 0.0015$ cm. The initial electron phase velocity has a standard deviation of $\sigma_G = 2.2$ and 4.2, where $\sigma_G = 4\pi N \Delta\gamma/\gamma$. The average initial phase velocity is centered around $\nu_0 = 0$. The electrons, in both scenarios, have bunched and are on the bottom-half in the separatrix at the end of the undulator, $\tau = 1$. The electrons have given energy to the optical field. The phase-space simulations indicate the production of an X-ray beam with saturation of the system at undulator lengths of 34 and 35

26

meters, respectively. The logarithmic power evolution shown in the upper right-hand corners of each figure indicate the systems have reached saturation. The peak power achieved for the 4.5 Å is approximately 66 GW and for the 1.5 Å it is approximately 11 GW.
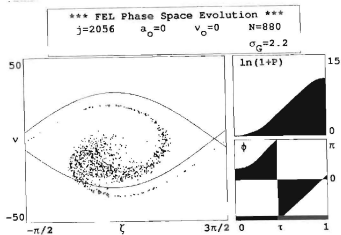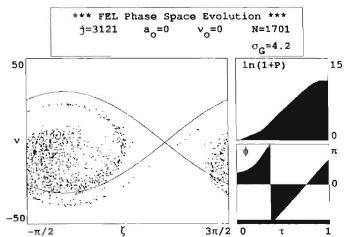

Figure 3-2. Phase-space plot for 4.5 Å system.

Figure 3-3. Phase-space plot for 1.5 Å system.

In either scenario, the proposed parameters would create a hard X ray FEL as indicated by the phase-space simulations. A large portion of the FEL cost is in the production of the undulator; reducing the length of the undulator reduces the FEL cost. A method of reducing the length of the undulator is by introducing a dispersive section in the undulator to make an FEL klystron. A penalty resulting from the klystron design is the onset of saturation at weaker fields than without the klystron [9].

B. KLYSTRONS AND HIGH-CURRENT HIGH-POWER FEL

An FEL with an optical wavelength of $\lambda = 40$ Å was proposed using the SLAC linac as an electron beam source [10]. Table 3-2 gives the original proposed parameters for the optical wavelength of $\lambda = 40$ Å. The system required an undulator with a length of 60 meters. The phase-space plot in Fig. 3-4 shows a simulation of a soft X-ray FEL at 40 Å using the parameters in Table 3-2, an initial radiation field $a_0 = 0$, and a phase velocity spread of standard deviation $\sigma_G = 3.6$ centered around $v_0 = 0$.

PARAMETERS	VALUE
λ (Radiation Wavelength)	40 Å
λ_0 (Undulator period)	8.3 cm
K (Undulator parameter)	4.2
Undulator type	Linear
ε_n (Normalized rms emittance)	3.0 mm-mrad
γmc^2 (Electron energy)	7.0 GeV
I (Peak current)	2500 A
Energy spread	0.0004
L (Undulator length)	60 m
Output power	28 GW

Table 3-2. Proposed parameters for a $\lambda = 40$ Å X ray FEL at SLAC.
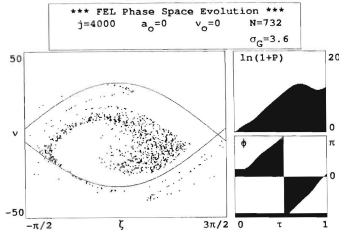(Without dispersive section)

Figure 3-4. Phase-space plot for 40 Å system.
(Without dispersive section)

The optical field grows from noise as a result of interaction with 200,000 electrons randomly positioned in the initial electron phase. The dimensionless current $j = 4000$ corresponds to a current $I = 2500$ A. Notice, at the end of the undulator, $\tau = 1$, the electrons have already reached saturation as shown in the power plot in the upper right diagram. Having gone through one complete transversal inside the separatrix, the bunched electrons are near the bottom of the separatrix, for a second time, where maximum energy transfer to the optical beam occurs. When the electrons are bunched at the upper half of the separatrix the electron beam has taken back energy from the optical beam as indicated by the drop of the optical power after the onset of saturation. Reducing the undulator length to approximately 40 m, at the onset of saturation, will result in peak power at the end of the undulator. The majority of electrons will be at the bottom of the separatrix and the electrons will have given up the maximum energy possible to the optical beam. By reducing the length of the undulator we reduce the dimensionless current, $j = 8\pi^2 e^2 \rho N K^2 L^2 F / \gamma^3 mc^2$. With an undulator length of 40 m, the dimensionless current is $j = 2000$. Figure 3-5 is the phase-space plot for such a system.

To reduce costs of manufacturing an undulator of such a long length and maintaining the same results, a dispersive section can be added to an undulator, thus

29

making a klystron. Table 3-3 lists the proposals for a system that uses a klystron to produce a 40 Å FEL [11].
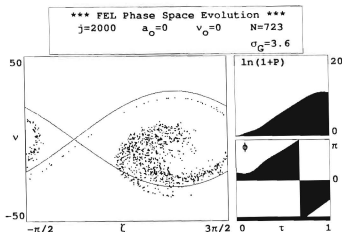

Figure 3-5. Phase-space plot for 40 Å system, undulator length of 40 m.

The FEL design at $\lambda = 40$ Å with a klystron has an undulator length of $L = 17$ meters, electron beam energy of 5 GeV, and a peak current of 5000 A, which corresponds to a dimensionless current density of $j = 932$. This FEL was examined without a klystron and then with a klystron.

The case without the klystron is shown in Fig. 3-6. The electron bunch is at a phase where it gives energy to the optical field at the end of the undulator. The dimensionless power P corresponds to a peak power of 15 GW. In Fig. 3-7, the use of the klystron FEL with the same parameters and $D = 0.5$ shows that electrons have bunched in the lower half of the separatrix and at the optimal phase relation $\zeta + \phi = \pi$ for maximum gain. The peak power calculated for the klystron FEL is 31 GW. While not shown, saturation will occur earlier with the use of a dispersive section than without, reducing the overall length of the undulator.

PARAMETERS	VALUE
λ (Fund. Rad. Wavelength)	40 Å
λ_0 (Undulator period)	4.0 cm
K (Undulator parameter)	4.2
Undulator type	Linear
ε_n (Normalized rms emittance)	3.0 mm-mrad
γmc^2 (Electron energy)	5.0 GeV
I (Peak current)	5000 A
Energy spread	0.0004
L Undulator length	17 m
Output power	2 GW

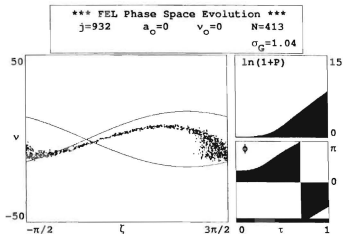Table 3-3. Proposed parameters for a λ = 40 Å X ray FEL,
(With dispersive section).

Figure 3-6. Phase-space plot for 40 Å X ray FEL,
(Without dispersive section).

To generalize the optical field in the longitudinal direction, several sites along the complex wave envelope, $a(z)$, are followed. The length in the z direction is scaled to the slippage distance $N\lambda$, the distance the electron pulse slips back relative to the optical pulse over one pass through the undulator. This is the distance over which the optical pulse and the electron beam interact. All longitudinal distances are normalized to this slippage distance so that $z/N\lambda \to z$. This then gives
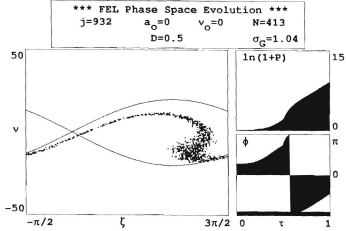

Figure 3-7. Phase-space plot for 40 Å X ray FEL,
(With dispersive section).

$a \to a(z)$, $v \to v(z)$, and $\zeta \to \zeta(z)$ over a number of sites. The pendulum and wave equation can be generalized to [3]

$$\frac{d^2\zeta_{z+\kappa}}{d\tau^2} = |a_z|\cos(\zeta_{z+\kappa} + \phi_z) \qquad (3.1)$$

and

$$\frac{da_z}{d\tau} = -j_{z+\kappa} < e^{-i\zeta_{z+\kappa}} >_{z+\kappa} , \qquad (3.2)$$

where the longitudinal field sites z refer to a position in the optical field envelope. When the electrons pass through the undulator they exchange information with the optical wave envelope in a range of sites. The optical light traveling at speed c, remains fixed in z. The slower electrons slip back to site $z - \tau$. Those electrons at

32

site z interact with a range of sites in the optical wave envelope. The electrons then pass information from one site to another.

Longitudinal multimode simulations shown in Fig. 3-8 and 3-9 using the same parameters as in Fig. 3.7 and 3.8, study the coherence development of the optical field. At the bottom-left of each simulation we see the gain over the undulator length. The bottom-middle is the single-mode gain spectrum as a function of frequency centered around resonance. The bottom right is the evolution of power developed through the undulator length, measured in a dimensionless power, corresponding to tens of GW. The middle-left plot is the growth in the optical field amplitude over two slippage distances in length, $-1 < z < 1$. The middle and top-middle show the evolution of the power spectrum. The triangle tick mark indicates resonance, $\nu = 0$ and the rectangle tickmark indicates ν of the electron beam at the end of the undulator. In the klystron undulator, the final power is much higher. The middle-right and top-right frames show the development of the electron phase velocity distribution. There is a decrease in the average electron phase velocity which corresponds to energy given up to the optical field. In the FEL without a klystron, little energy is given up to the optical beam, while the system with a klystron gives up significantly more energy. The simulation without a klystron and before saturation resulted in an X-ray linewidth of $\Delta\lambda/\lambda \approx 0.1\%$, where $\Delta\lambda/\lambda = \Delta\nu/2\pi N$ and N is the number of periods in the undulator. Adding a dispersive section does not change the linewidth. There is no degradation to the quality of the optical beam.

In these systems the standard deviation of phase velocity was $\sigma_G = 1.04$. As the standard deviation of the phase velocity increases it makes it difficult for the electrons to bunch. Tin phase velocity, σ_G, must be considered when using a klystron FEL.
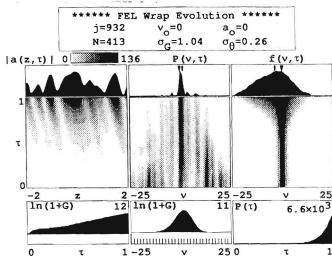
****** FEL Wrap Evolution ******
j=932 v_o=0 a_o=0
N=413 σ_G=1.04 σ_θ=0.26

Figure 3-8. Longitudinal multi-mode simulation for 40 Å X ray FEL,
(Without dispersive section).

****** FEL Wrap Evolution ******
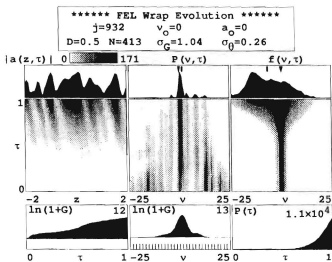j=932 v_o=0 a_o=0
D=0.5 N=413 σ_G=1.04 σ_θ=0.26

Figure 3-9. Longitudinal multi-mode simulation for 40 Å X ray FEL,
(With dispersive section).

34

C. PHASE VELOCITY SPREADS AND KLYSTRONS

As mentioned in Section II.E, for a change in initial energy $\Delta \gamma mc^2$, there is a corresponding change in electron phase velocity, $\Delta v \approx 4\pi N \Delta \gamma / \gamma$, in which the Gaussian distribution of energies with an rms spread , $\Delta \gamma / \gamma$, characterizes the standard deviation $\sigma_G = 4\pi N \Delta \gamma / \gamma$. When $\sigma_G \approx \pi$, bunching becomes impaired. The use of a klystron to bunch the electrons may not have a positive effect if the electron energy spread is so large that the modulator cannot develop the phase velocity differences to prepare the electrons for bunching. Figures 3-10a, 3-10b, 3-10c, and 3-10d are plots on how the standard deviation in energy spread can effect the use of a klystron undulator at three different dimensionless current.

Figures 3-10a, 3-10b, and 3-10c show what happens with various energy spreads on high-current systems ($j = 10000$, $j = 2200$, and $j = 500$). Figure 3-10d is the plot for low-current system ($j = 1$).

In all four figures you can see as the energy spread, σ_G, increases, the overall gain of the system decreases. By using a klystron undulator it is hoped to increase the gain by at least double the magnitude compared to the case where a klystron was not used. With a high σ_G, it is apparent from the figures that a klystron will not produce a gain significant enough to warrant its use. The use of a klystron at the high σ_G (2.0 and 3.14) may even cause a decrease in gain. In the monoenergetic beam ($\sigma_G = 0.0$), there is no limit to the strength of the dispersive section or to the gain of the system; but, this is unrealistic. The plots indicate that a moderate spread, $0.0 < \sigma_G < 1.5$, can be compensated for in a klystron and provide a significant gain that would warrant its use. The magnitude of D is critical though. If D is to large it may have a negative effect and cause the system to decrease in gain. It is also shown that as the dimensionless current is increased the critical size of D also increases. A lower j can mean a lower D, the distance for the electrons to travel to bunch adequately is smaller in the lower energetic beam.

It was noted that for the 4.5 Å and the 1.5 Å lasers that SLAC has proposed the initial electron phase velocity has a standard deviation of $\sigma_G = 2.2$ and 4.2. The strength of the dispersive section thus becomes critical.
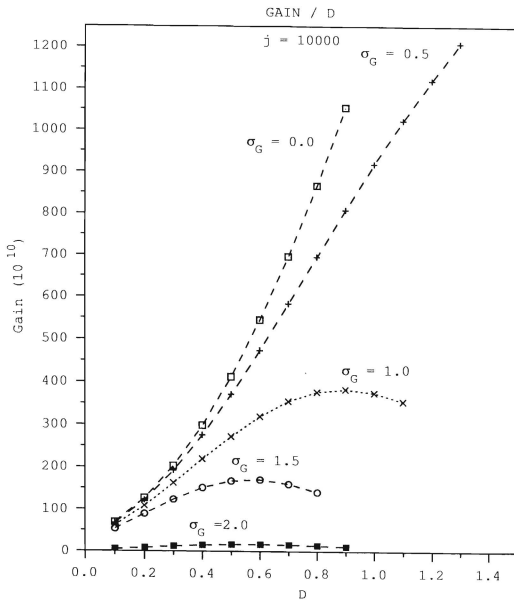
Figure 3-10a. Gain vs. D plots for dimensionless current j = 10000.
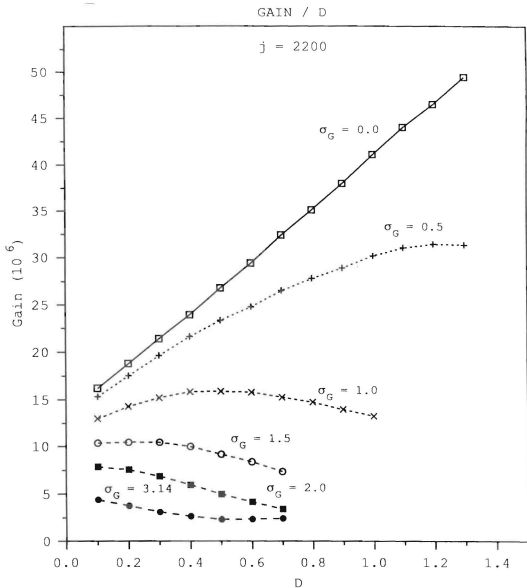
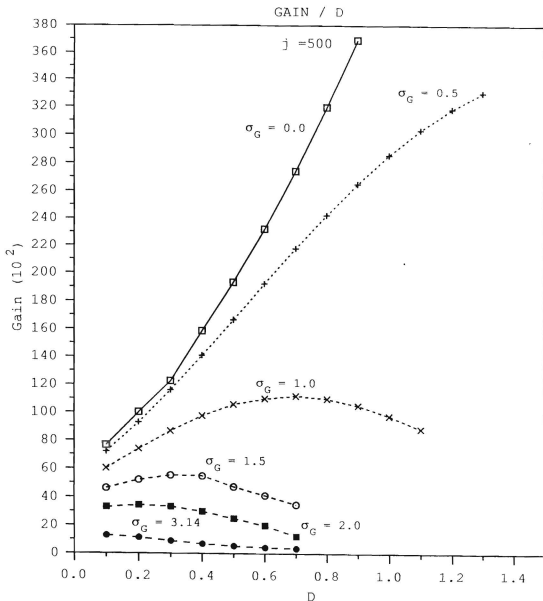Figure 3-10b. Gain vs. D plots for dimensionless current j = 2200.

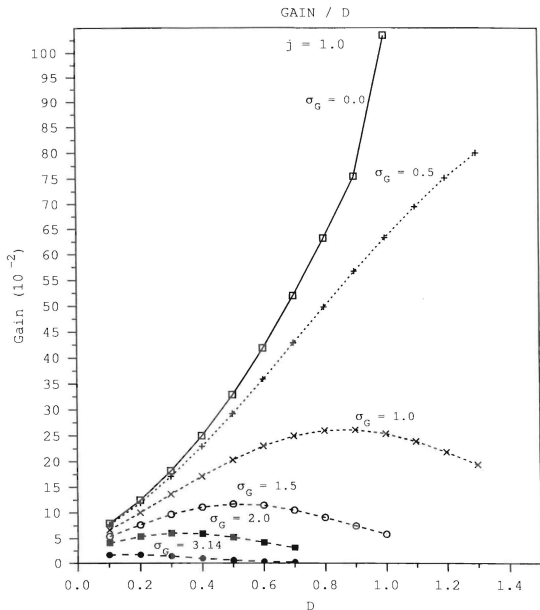Figure 3-10c. Gain vs. D plots for dimensionless current j = 500.

Figure 3-10d. Gain vs. D plots for dimensionless current *j* = 1.

39

D. 1.5 Å FEL WITH A KLYSTRON

The use of a dispersive section to shorten the length of a high power FEL such as proposed at SLAC would reduce the cost of the system. The linac is already in place, therefore the cost to build the FEL is largely in the manufacturing of an undulator. Shortening the undulator would reduce its cost significantly since the manufacturing of undulator sections is large.

To achieve significant gain in the 1.5 Å FEL, the strength of a dispersive section for $j = 3121$ and $\sigma_G = 4.2$ is estimated to be 0.2 from Fig. 3-10b. With high current, the maximum gain of an FEL is obtained when ν_0 is slightly off resonance. When adding a dispersive section to the undulator, the maximum gain is shifted to a higher value of ν_0, where $\nu_0 \approx \pi/2D$. The optimum for this system is found to be $\nu_0 \approx 4.0$.

Figure 3-11 is the phase-space plot for a 1.5 Å FEL with a length of 30 m, a dispersive strength of $D = 0.2$, $j = 2170$, $\sigma_G = 3.8$, and $\nu_0 \approx 4$. The length of the FEL was shortened from 35 m to 30 m which in turn lowered j and σ_G. The phase-space plot shows the system saturating at the end of the undulator. The peak power out is 14 GW, which is slightly higher than the simulation run without a dispersive section. All indications show that a dispersive section can be effective in shortening the length of the undulator and increasing gain.

In order to examine the coherence development, we look at a longitudinal multi-mode simulation in Fig. 3-12. We can see in the middle window a narrow spike indicating a narrow band width of $\Delta\lambda/\lambda = .1\%$, which indicates good coherence development. The right window shows an average decrease in electron phase velocity which corresponds to the electrons giving up energy to the optical beam, creating high optical power.

All the simulations that were run show that a dispersive section may have a positive affect in shortening the length of the undulator. The use of a dispersive section may decrease the cost of the FEL to be built by SLAC.
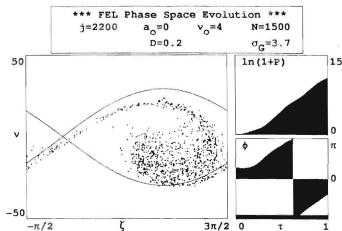
Figure 3-11. Phase-space plot for 1.5 Å system, undulator length of 30 m.
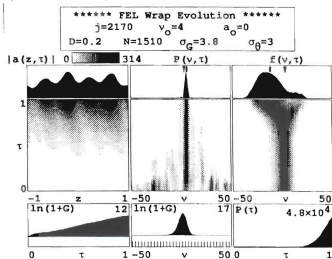
(With dispersive section)

Figure 3-12. Longitudinal multi-mode simulation for 1.5 Å X ray FEL.

(With dispersive section).

41

IV. CONCLUSIONS

The theory that has been presented is not limited to X ray FELs, but to all FELs. The Free Electron Laser has many uses in the military and industrial applications; ranging from high-power, speed-of-light self-defense weapon systems to DNA-pair imaging. The ability of an FEL to be tunable allows it to overcome limitations that other high powered lasers face, such as atmospheric effects. The FEL as a self defense weapon system does not require replenishment from a limited magazine. The FEL is a system that is needed in the present day military to overcome conditions that have outgrown systems now in use. There is a need for the United States to be the leader in laser technology to ensure its capability to improve world conditions.

The proposed SLAC X-ray FEL, which will come on-line in the near future, will be the first coherent X ray light source. The acquired technology is not limited to the SLAC proposal, but can be used to develop other types of high powered FELs. An injector system now under development for the SLAC linac will enable it to produce a 4.5 Å or 1.5 Å FEL.

The use of a dispersive section will aid in shortening the length of the undulator. A significant part of the cost to build the FEL at SLAC is manufacturing the undulator, so shortening of the undulator is economically important. However, beam quality must be high in order to use a dispersive section. So the cost of improving the injected electron beam quality must be considered in the decision to use a klystron undulator. The better the quality of the electron beam the greater the positive affects a dispersive section may have on increasing gain and shortening the overall length of the system.

Finally, we have presented simulation results to show that use of dispersive sections is a possible and potential cost-saving option. Further investigation in the use of dispersive sections on high-gain FELs is required. For example, positioning the dispersive section along the undulator to optimize its effects may be studied.
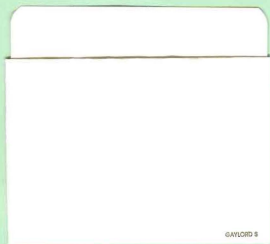
LIST OF REFERENCES

1. N. Bloembergen, and others, "Report to the American Physical Society of the Study Group on Science and Technology of Directed Energy Weapons", Reviews of Modern Physics, v.59, No.3, Part II, July 1987.

2. W.B. Colson, C. Pellegrini, A. Renieri and J.M.J. Madey, "Introduction To Free Electron Lasers," Chapter 1 in Free Electron Laser Handbook, W.B. Colson, C. Pellegrini and A. Renieri (eds.), North-Holland Physics, Elsevier Science Publishing Co. Inc., The Netherlands, 1990.

3. W.B. Colson, "Classical Free Electron Laser Theory," Chapter 5 in Free Electron Laser Handbook, W.B. Colson, C. Pellegrini and A. Renieri (eds.), North-Holland Physics, Elsevier Science Publishing Co. Inc., The Netherlands, 1990.

4. W.B. Colson, "Free Electron Laser Theory", Ph.D. Dissertation, Stanford University, September 1977.

5. W. B. Colson and A.M. Sessler, "Free Electron Lasers", Annual Reviews of Nuclear and Particle Science, v.35,pp. 25-54,1985.

6. W. B. Colson, J.C. Gallardo, and P.M. Bosco, "Free-Electron-Laser Gain Degradation and Electron-Beam Quality", Physical Review Letters, A34, No.6,pp. 4875-4881, December 1986.

7. "Workshop on Scientific Applications of Short Wavelength Coherent Light Sources",SLAC-414, SLAC/SSRL-0007, CONF-9210278, 1993.

8. "Notes on LCLS Technical Group Meeting", SLAC/SSRL-01, July 27,1994

9. G.H. Winter, J. Hall, R.K. Wong and W.B. Colson, "Simulations of a Klystron Undulator for the SLAC X-ray FEL", Nuclear Instruments and Methods in Physics Research, A358, pp. 68-69, 1995.

10. C. Pellegrini, et al., "A 2 to 4 nm Power FEL on the SLAC LINAC", Nuclear Instruments and Methods, A331, pp. 223-227,1993.

11. Joseph Barry Hall, "Simulations of an FEL Producing Coherent X Rays Utilizing The SLAC LINAC", Master's Thesis, Naval Postgraduate School, Monterey, CA, June 1994.

INITIAL DISTRIBUTION LIST